Since January 2020 Elsevier has created a COVID-19 resource centre with free information in English and Mandarin on the novel coronavirus COVID-19. The COVID-19 resource centre is hosted on Elsevier Connect, the company's public news and information website.

HOSTED BY

ELSEVIER

CrossMark

Available online at www.sciencedirect.com

ScienceDirect

Radiology of Infectious Diseases 2 (2015) 40–46

www.elsevier.com/locate/jrid

Research article

Longitudinal changes of pneumonia complicating novel influenza A (H1N1) by high-resolution computed tomography

Feng Feng [a,b,*], Ganlin Xia [b], Yuxin Shi [a,**], Zhiyong Zhang [a,**]

[a] Department of Radiology, Shanghai Public Health Clinical Center, Fudan University, Shanghai, China
[b] Department of Radiology, Nantong Tumor Hospital, Nantong University, Nantong, Jiangsu Province, China

Received 30 October 2014; accepted 27 February 2015
Available online 9 June 2015

Abstract

Purpose: To assess lung lesions in patients with pneumonia complicating novel influenza A (H1N1) by serial high-resolution computed tomography (HRCT) during the early, progressive and convalescent stages.
Samples and methods: Serial HRCT scans in 39 patients with pneumonia complicating novel influenza A (H1N1) were reviewed for predominant patterns of lung abnormalities as well as distribution and extent of involvement. Longitudinal changes were assessed at different time points.
Results: In the early stage, the most common HRCT finding was patchy ground-glass opacity (GGO) (n = 4, 54.7%). In the progressive stage, bilaterally distributed GGO mixed with consolidation was the most commonly observed feature (n = 28, 71.8%). The diffuse pattern deteriorated to a peak (n = 17, 43.6%) at this stage. In the convalescent stage, the most common finding was fibrosis (n = 25, 64.1%). Averagely, fibrosis was observed at d 18.5 ± 6.4 after the onset of symptoms. Three patterns of longitudinal changes of the lesions were observed, including: type 1, improvement after deterioration; type 2, concurrent improvement and deterioration followed by improvement; and type 3, gradual improvement. Type 1 was the more common pattern (n = 27, 69.2%). Complete serial HRCT scans from initial and final scan were obtained in 24 patients, and the mean CT score peaked at d 8–14 of the illness.
Conclusion: HRCT may play a role in detecting and characterizing pulmonary lesions for the cases of pneumonia complicating influenza A. In addition, it may contribute to monitoring longitudinal changes of pneumonia and assessing therapeutic response.

Keywords: H1N1; High-resolution computed tomography; Influenza; Lung

1. Introduction

A new strain of influenza A virus, H1N1, was firstly recognized in early 2009 after its first worldwide pandemic [1]. Although initial reports suggested that the condition associated with pandemic influenza A (H1N1) in 2009 might be milder compared to the influenza pandemic in 1918, characteristic clinical data and high-risk populations of its complications are still of great clinical significance [2]. The most common clinical findings of H1N1 virus infection include fever, cough, dyspnea, fatigue, myalgia, and headache. In most cases, the symptoms are mild and self-limited. However, a small percentage of patients with influenza A (H1N1) develop severe pneumonia that may progress into respiratory failure that occasionally requires mechanical ventilation, and even death [3–5].

The predominant CT findings in patients with influenza A (H1N1) complicated by pneumonia are ground-glass opacities (GGOs), areas of consolidation, or a mixed pattern of GGOs and consolidations [6,7]. Bilateral, multifocal or diffuse consolidation, often associated with GGOs, is the predominant CT finding in patients with more severe clinical condition of

* Corresponding author. Department of Radiology, Shanghai Public Health Clinical Center, Fudan University, Shanghai, China. Tel.: +86 21 37990333 7335; fax: +86 21 57247094.
** Corresponding authors. Tel.: +86 21 37990333 7335; fax: +86 21 57247094.
E-mail addresses: drfengfeng@163.com (F. Feng), shiyuxin@shaphc.org (Y. Shi), zhangzy@shaphc.org (Z. Zhang).
Peer review under responsibility of Beijing You'an Hospital affiliated to Capital Medical University.

http://dx.doi.org/10.1016/j.jrid.2015.06.001

influenza infection [8,9]. Thin-section CT, particularly high-resolution CT (HRCT), in the documentation of parenchymal abnormalities in influenza A (H1N1) when chest radiographs demonstrate normal or only questionable abnormalities has also been established. CT also facilitates assessing complications and providing evidence of mixed pulmonary infections in patients who fail to respond to appropriate therapy [10]. Limited data are available, however, on sequential CT findings during the subsequent course of influenza A (H1N1), especially regarding sequelae that may occur during convalescence [11,12]. Thin-section CT evidence of fibrosis during the convalescent stage has recently been reported in patients with influenza A (H1N1) [12]. Thus, the purpose of our study was to evaluate the lung parenchymal abnormalities in patients with influenza A (H1N1) by serial HRCT scans at the early, progressive and convalescent stages of the disease.

2. Samples and methods

Our research protocol was approved by the Research Review Board of our institution. All patients with clinically proven pneumonia complicating influenza A (H1N1) who were admitted to the Clinical Center of Public Health in Shanghai, China between July 2009 and March 2011 were enrolled as the subjects of the study. All of the patients underwent at least three serial HRCT chest scans. Specifically, a total of 39 patients (aged 19–78 years with a mean of 42.2 years), including 27 males and 12 females, participated in the research. Their diagnoses of pneumonia complicating influenza A (H1N1) were defined by the National Center for Disease Control and Prevention, China. Oropharyngeal and/or nasopharyngeal specimens of all patients were examined using real-time polymerase chain reaction (RT-PCR), all of which showing positive to H1N1 virus strain. To avoid unnecessary exposure to radiation, HRCT should be reserved for patients whose diagnosis is uncertain or for patients with clinical deterioration that requires further evaluation of lung abnormalities. For patients with highly suspected concurrent infections, additional microbiological examinations for other viral, bacterial and fungal infections are recommended. All patients experienced fever with a body temperature of above 38 °C, tachypnea, and cough. Other common symptoms included generalized weakness (n = 18, 46.2%) and headache (n = 9, 23.1%). Preexisting medical conditions were reported in 19 (48.7%) patients, including pregnancy (n = 2, 5.1%), primary hypertension (n = 12, 30.8%), chronic hepatitis B (n = 2, 5.1%), ankylosing spondylitis (n = 1, 2.6%), lymphoma (n = 1, 2.6%), and type II diabetes (n = 1, 2.6%). All the patients received neuraminidase inhibitors (oseltamivir), while 21 (53.8%) also received corticosteroids. Mechanical ventilation was performed for 12 (30.8%) patients. And no occurrence of death was reported in our study.

At admission, within 1–7 days after the onset of symptoms, the findings of laboratory tests included evaluated WBC count in 5 cases (7.9%), decreased WBC count in 18 cases (46.2%), decreased PO_2 level in 25 cases (64.1%), decreased CD4+ T cell count in 36 patients (92.3%), and increased C-reaction protein level in all 39 patients (100%).

CT scans were performed with a 16-slice Siemens CT scanner (Somatom Sensation 16, Erlangen, Germany) using the volumetric technique and no contrast enhancement. Spiral scans were obtained with the same scanner under the following parameters setting: 110 mAs, 120 kVp, 0.75-mm collimations, 1 mm slice, and a high-spatial-frequency reconstruction algorithm. All images were reviewed at a picture archiving and communication system workstation. The images were obtained with both mediastinal (width 350–450 HU and level 20–40 HU) and parenchymal (width 1200–1600 HU and level −500 to −700 HU) window settings. Two experienced radiologists working in the field of chest radiology for 12 and 22 years reviewed the HRCT scans independently and any disagreement was reached consensus after discussion to a final interpretation.

The predominant patterns of lung abnormalities on the HRCT scans were classified as GGO, consolidation, and mixture of GGO and consolidation. The HRCT scans were assessed for the presence and distribution of GGOs and consolidations. GGO was defined as hazy area of increased attenuation that did not obscure the underlying vessels. Consolidation was defined as homogeneous opacification of the parenchyma that obscured the underlying vessels. Parenchymal band was defined as non-tapering linear opacity that was several millimeters thick and several centimeters long. Reticular opacity was defined as linear opacities arranged into a network. The presence of a parenchymal band, reticular opacities, traction bronchiectasis, or irregular interfaces (bronchovascular, pleural, or mediastinal) was considered to be evidence of fibrosis [13]. On the scans, the presence of mediastinal lymphadenopathy (defined as a lymph node with 1 cm short-axis diameter), pneumothorax, and pleural effusion was also noted. The distribution of abnormalities was categorized as focal, multifocal, and diffuse. A focal distribution was defined as a singular focus of abnormality. A multifocal distribution was defined with more than one focus and was further classified into unilateral and bilateral. A diffuse distribution was defined as bilateral abnormalities with an equivalent volume of one or both lungs involved.

All HRCT scans were categorized according to the time points of scanning, including the day of symptoms onset as well as the days on which the scan was obtained such as day(d) 1–3, d 4–7, d 8–14, d 15–21, d 22–28 and after d 28 since the symptoms onset. The initial and follow-up scans were analyzed to determine longitudinal changes of the detected main lung abnormalities. The patterns, extent and distribution of the abnormalities were compared with findings in the same region on previous and subsequent HRCT scans.

Patients undergoing initial and all follow-up scans within a minimum of 21days were enrolled for further analysis to determine longitudinal changes of the detected main lung abnormalities.

The extent of involvement of each abnormality was assessed independently for each of three zones: upper (above the carina), middle (below carina and above the inferior

pulmonary vein) and lower (below the inferior pulmonary vein). Each lung zone (totally 6 lung zones) was assigned a value based on the following criteria: 0 for no involvement, 1 for involvement of less than 25%, 2 for involvement of 25–50%; 3 for involvement of 50–75%, and 4 for involvement of above 75%. Sum of the values indicates the overall lung involvement and the maximal CT score was then 24.

3. Results

The patterns, extent and distribution of the lung abnormalities by HRCT scans at different time points were listed in detail in Table 1. Serial HRCT scans of 39 patients were categorized into the early, progressive, and convalescent stages. No scans demonstrated nodules or mediastinal lymph nodes at any time point of assessment.

At the early stage, chest HRCT was performed in 7 patients within 3 days after symptoms onset. Patchy GGO with homogeneous density, segmental distribution and poorly defined boundary were shown in 4 cases. In addition, mixture of patchy GGOs with consolidations was present in 3 cases.

In the progressive stage, chest HRCT was performed in all 39 patients within d 4–7 and d 8–14 after the symptoms onset. The lesions of the 7 patients who received HRCT scan at the early stage progressed at d 4–7. The lesions of 39 patients deteriorated to a peak during d 8–14. The HRCT abnormality peaked averagely at d 9.8 ± 2.1 after the symptoms onset. Mixture of bilaterally distributed consolidations with GGOs was the most commonly observed pattern (n = 28, 71.8%). The diffuse pattern deteriorated to a peak abnormality rate (n = 17, 43.6%). During d 4–14 of assessment, confluent air-space opacities diffusely involved both lungs, compatible with acute respiratory distress syndrome (ARDS) (Fig. 1), in 4 cases (10.3%). Pneumothorax was noted in 1 patient at d 6 after the onset. Three patients developed super-infection, and 2 of these patients developed aspergillus. By HRCT for one patient, progressive consolidation was noted; and for another, a cavity was noted in the right upper lung. And one patient developed staphylococcal septicemia with multiple cavities in both lungs by HRCT scanning (Fig. 2).

In the convalescent stage, the extent of lesions in lungs of 5 patients gradually decreased since d 7 after symptoms onset, and improved after d 14 in another 32 patients. A predominant pattern of consolidation with or without GGO was the most common during the first 14 days and decreased thereafter. Serial HRCT scans obtained in 25 patients demonstrated fibrosis, including 7 cases during d 8–14 and 18 cases after d 14. The prevalence of fibrosis decreased slowly thereafter. Averagely, fibrosis was observed at d 18.5 ± 6.4, either confined within the subpleural region of lungs or diffusing from the subpleural region. In 24 patients, final HRCT scan was obtained at d 22–28 or after d 28. The lesions in 5 (20.8%) patients were completely absorbed, and the extent of lesions in 19 patients (79.2%) decreased. Residual fibrosis was observed in 16 patients (66.7%), and one patient showed residual fibrosis only at the dorsal lower lobes at d 97 after the symptoms onset.

Three patterns of longitudinal changes of the lung lesions were identified: type 1, improvement after deterioration (Figs. 1 and 2); type 2, concurrent improvement and deterioration followed by improvement; and type 3, gradual improvement (Fig. 3). Type 1 was the most common pattern (n = 27, 69.2%). The involvement and distribution of lesions were noted, including unilateral or bilateral, singular or multiple segments/lobes involved, diffuse or focal distribution. Type 2 was the second most common pattern (n = 7, 17.9%). The lesions were found completely absorbed or decreased. However, new lesions may be present and were then absorbed. Type 3 was observed in 5 patients (12.8%). Multifocal or diffuse opacities were present within d 4–7 and were gradually absorbed as shown by follow-up HRCT scans.

A total of 24 patients received all serial HRCT scans. The patterns, extent, distribution and mean CT scores of the lung lesions by HRCT scans at different time points were shown in detail in Table 2. The estimated mean CT scores peaked at d 8–14 of the illness course, indicating a marked increase of severity at d 8–14, with a slow decrease thereafter (Fig. 4).

Table 1
Pattern, severity and distribution of lung lesions by HRCT at the different time points.

	1–3 d (n = 7)	4–7 d (n = 39)	8–14 d (n = 39)	15–21 d (n = 29)	22–28 d (n = 16)	>28 d (n = 8)
Abnormal CT findings						
GGO	4(57.1)	10(25.6)	5(12.8)	4(13.8)	2(12.5)	2(25)
Consolidation	0(0)	4(10.3)	6(15.4)	3(10.3)	1(6.3)	0(0)
Mixed	3(42.9)	25(64.1)	28(71.8)	15(51.7)	5(31.3)	1(12.5)
Fibrosis	0(0)	0(0)	7(17.9)	19(48.7)	11(68.8)	5(62.5)
Pleural effusions	0(0)	4(10.3)	9(23.1)	4(13.8)	0(0)	0(0)
Distribution						
Unilateral	2(28.6)	0(0)	0(0)	0(0)	1(6.3)	1(12.5)
Bilateral	5(71.4)	39(100)	39(100)	29(100)	12(75.0)	5(62.5)
Severity						
Focal	1(14.3)	0(0)	0(0)	0(0)	0(0)	1(12.5)
Multifocal	6(85.7)	28(71.8)	22(56.4)	21(72.4)	12(75.0)	5(62.5)
Diffuse	0(0)	11(28.2)	17(43.6)	8(27.6)	1(6.3)	0(0)

The numbers in parentheses indicate percentages. HRCT, high-resolution computed tomography; GGO, ground-glass opacity; Mixed, mixture of GGOs and consolidations.

4. Discussion

The serial HRCT scans obtained in our cohort provided an opportunity to study the longitudinal changes of lung abnormalities in patients with pneumonia complicating influenza A (H1N1) at its early, progressive and convalescent stages. These heterogeneous scans were obtained to facilitate clinical management. Nevertheless, the scans depicted the lung abnormalities at specific time points from the symptoms onset and allowed for a description of temporal lung changes in such a condition.

At the early stage, the primary HRCT finding is focal or multifocal GGO. Otherwise, a combination of patchy GGOs and consolidations is the predominant finding that bilaterally affects the lung lobes. The most common HRCT finding was

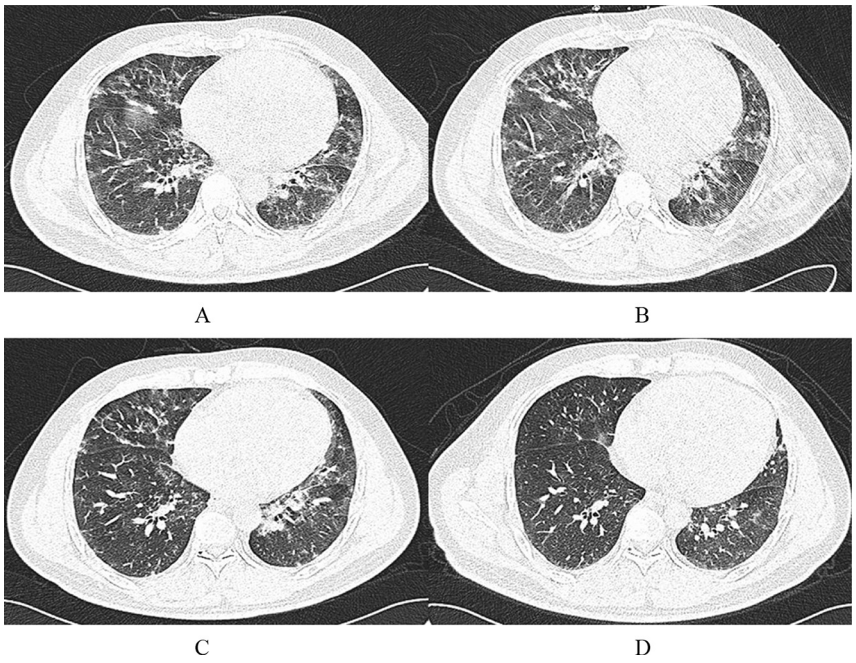

Fig. 1. HRCT scans in a 40-year-old man with ARDS due to influenza A (H1N1) pneumonia. A.A scan obtained at d 6 of illness showed bilaterally diffuse GGOs. Due to progression of symptoms, he was admitted to the ICU at d 6 of illness for mechanical ventilation. B. A scan obtained at d 9 of illness showed progression of GGOs. C. A scan obtained at d 15 of illness showed GGOs were improved. D. A scan obtained at d 34 of illness showed GGOs were almost resolved.

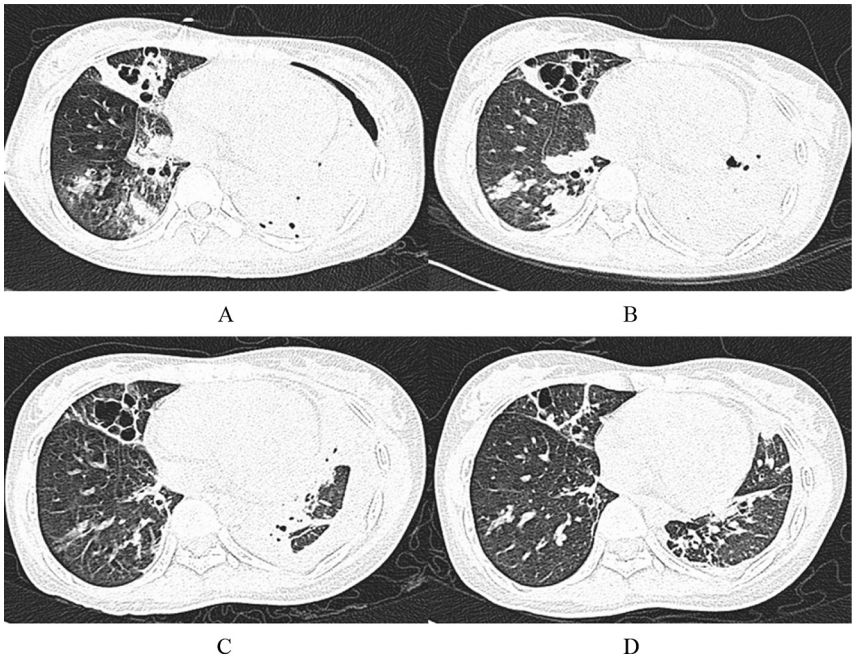

Fig. 2. HRCT scans in a 23-year-old woman with influenza A (H1N1) pneumonia and secondary staphylococcal septicemia. A. An HRCT scan obtained at d 6 of illness showed bilateral consolidations in the mid and lower lung zones, and multiple cavities in the right middle lung lobe. Left pneumothorax was observed. B. A scan obtained at d 13 of illness showed enlarged cavities and progression of consolidations. The left pneumothorax was resolved. C. A scan obtained at d 18 of illness showed that consolidations were gradually absorbed and linear opacities developed in the previously consolidated regions, but the cavities persisted. D. A scan obtained at d 26 of illness showed that the consolidations were gradually absorbed and the cavities were improved.

patchy GGO (n = 4, 54.7%), which can be generally attributable to thickened alveolar septa in regardless of its association with partial airspace filling [14]. No patient was found with centrilobular nodules or tree-in-bud opacities in our cohort, possibly because our subjects were primarily hospitalized patients that most likely represent those with severe condition at the disease spectrum. It has been speculated that relatively rare involvement of the small airways may be

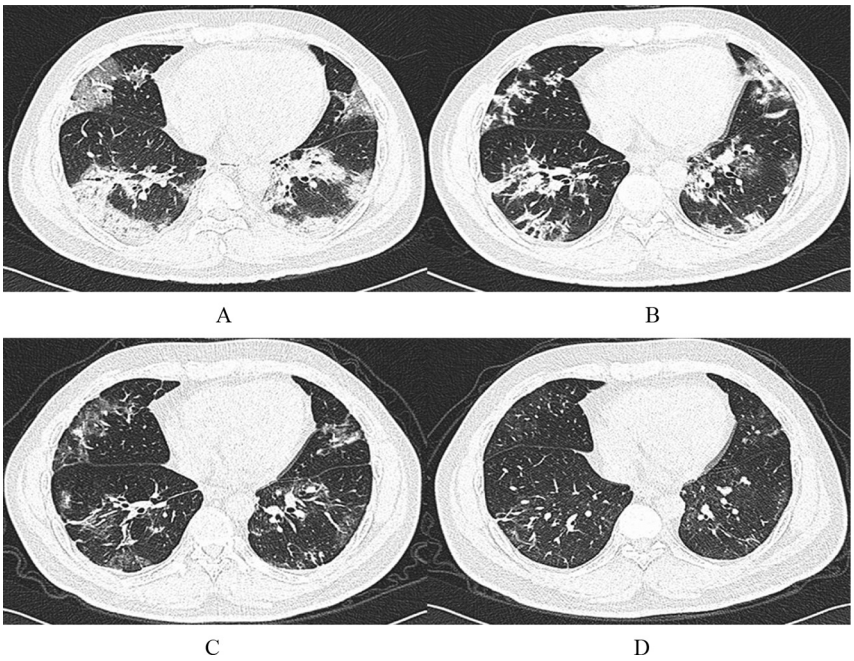

Fig. 3. HRCT scans in a44-year-old man with influenza A (H1N1) pneumonia. A. A scan obtained at d 7 of illness showed the multifocal consolidations in both lower lung lobes and patchy subpleural GGOs in both middle lung lobes. B. A scan obtained at d 14 of illness showed the mixed lesions were absorbed, with parenchymal bands in both lungs. C. A scan obtained at d 21 of illness just before discharge showed gradually absorbed abnormalities. D. A scan obtained at d 97 of illness showed residual subpleural fibrosis in both lower lung lobes.

caused by radiological procedure of severe infection in its clinical course when diffuse alveolar damage obscures the abnormalities of the airways. Yuan et al. [15] reported centrilobular nodules are present in 30 (45.5%) patients with mild symptoms, which is the second most common finding on HRCT. In addition, Elicker et al. described small airway involvement manifested as centrilobular nodules and tree-in-bud opacities, which is the most common radiological finding in the immunocompromised population [16].

In the progressive stage, the parenchymal lesions often develop from focal or multifocal areas to multifocal or diffuse areas during the radiological follow-ups. In the present study, the abnormality peaked at a mean of d 9.8 ± 2.1 from the symptoms onset by HRCT. During d 8–14, all 39 patients presented with multifocal or diffuse lesions in both lungs, and some of the diffuse lesions further progressed to a peak (n = 17, 43.6%). Consolidation with or without GGO was the most common HRCT finding (n = 28, 71.8%). Previous radiological reports of pneumonia complicating have shown poorly defined patchy areas of air-space consolidation with a diameter of 1–2 cm, which develop rapidly into confluence. These radiological findings indicate concurrence of diffuse alveolar damage, hemorrhage and organizing pneumonia,

Table 2
Patterns, severity, distribution and scores of lung lesions in the 24 patients at the different time points.

	1–7 d (n = 24)	8–14 d (n = 24)	15–21 d (n = 24)	>21 d (n = 24)
Abnormal CT findings				
GGO	7(29.7)	5(20.8)	4(16.7)	4(16.7)
Consolidation	1(4.2)	3(12.5)	3(12.5)	1(6.3)
Mixed	16(66.7)	16(66.7)	13(54.2)	8(33.3)
Fibrosis	0(0)	3(12.5)	12(50.0)	16(66.7)
Pleural effusions	2(8.3)	5(20.8)	3(12.5)	0(0)
Distribution				
Unilateral	0(0)	0(0)	0(0)	1(6.3)
Bilateral	24(100)	24(100)	24(100)	17(70.8)
Severity				
Focal	0(0)	0(0)	0(0)	1(0)
Multifocal	18(75.0)	13(54.2)	20(88.3)	17(70.8)
Diffuse	6(25.0)	11(44.8)	4(11.7)	1(4.2)
Mean CT Scores	8.8 ± 3.6	11.0 ± 4.7	8.2 ± 3.6	5.1 ± 3.1

The numbers in parentheses indicate percentages. GGO, ground-glass opacity; Mixed, mixture of GGOs and consolidations.

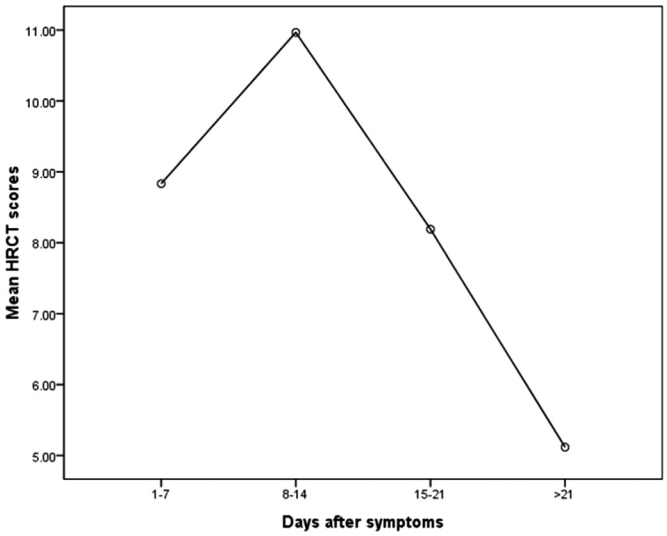

Fig. 4. Line graph showed mean HRCT scores at various time points after onset of symptoms. The scores peaked at d 8–14 of illness, with a decline thereafter.

possibly with superimposed secondary bacterial infection at its progressive stage [17]. In our study, superimposed bacterial or fungal infection of the respiratory tract was observed in 3 patients. Viral pneumonia complicated by a secondary infection presents a challenge in therapy choosing. For the cases with cavitation by HRCT, the condition may progress due to co-infection, such as aspergillus or staphylococcal septicemia, which indicates appropriate treatment. In addition, diffusely confluent air-space opacities with both lungs involved by HRCT may be indicative of acute respiratory distress syndrome (ARDS) [18]. ARDS may be present with respiratory epithelial injury with abnormally increased permeability of the capillary endothelium that initially produces patchy GGOs on HRCT and further evolves to confluent bilateral air-space opacity. In our study, the pattern was exhibited in 4 patients with ARDS.

In the convalescent stage, the predominant pattern of consolidation with or without GGO within d 1−14 after symptoms onset began to decrease, but fibrosis kept to progress. These findings indicated that persistent lung abnormalities in patients with pneumonia complicating influenza A (H1N1) may suggest the development of fibrosis, although GGOs or consolidations are largely reversible in such cases. In the present study, the lesions in 5 patients (12.8%) resolved completely, while signs of fibrosis were observed in 25 patients (64.1%). Fibrosis was observed averagely at d 18.5 ± 6.4 after the onset of symptoms. The patients who were detected signs of fibrosis were observed to recover over time. These findings are in agreement to those by Li et al. [12], who reported serial CT scans of 70 patients with influenza A after treatment. In their report, fibrosis developed in the first week and peaked at the third week. Thereafter, the lesion began to decrease slowly. Pathologically, fibrosis can be observed at the later stages of influenza A infection [19,20]. Gill et al. [21] described the pathological findings of lungs after autopsy of 34 death cases from influenza A (H1N1) infection. They reported that 2 had fibrosis, with an average hospitalization for 31.5 days. As far as we know, fibrosis is caused by activated fibroblast and deposited collagen [18]; and lung lesion, correlated with a restrictive defect, is characterized by a reticular appearance, parenchymal distortion and traction bronchiectasis mostly with ventral distribution. It is worth noting that residual fibrosis in 1 patient of our study remained in the basal and peripheral lung regions at d 97. And the finding resembles to that in patients with severe acute respiratory syndrome (SARS). Patients with SARS have been demonstrated with pulmonary fibrosis 6 months after the initial diagnosis by thin-section CT scanning [22,23].

We described longitudinal changes of lung abnormalities demonstrated by HRCT in 39 patients with clinically defined pneumonia complicating influenza A (H1N1) at its early, progressive and convalescent stages. In contrast to the patients with mild conditions reported by Yuan et al., [15] all 9 patients showed alleviation after 4 days of standard antiviral therapy, and 6 were close to cure. However, in our study, the duration of disease was longer than those reported by Yuan et al. And the longitudinal changes of lung abnormalities in our study were different and complex. The group of patients in our study more likely represents severe condition of pneumonia complicating influenza A (H1N1), which is more common in individuals with concomitant chronic disease. In the present study, 19 patients (48.7%) reported preexisting medical conditions. The longitudinal changes of lung lesions demonstrated by serial HRCT can be divided into 3 types: improvement after deterioration, improvement and deterioration followed by improvement, and gradual improvement. And the type of improvement after deterioration is the most common (n = 27, 69.2%). Totally, 24 patients did not miss any HRCT scans, showing marked deterioration of the lesions at d 8−14 by a peak of estimated mean CT score during this period as well as slow improvement thereafter. Li et al. reported similar findings, but they failed to classify the longitudinal changes of the lung lesions [12]. After we gain knowledge about the dynamic evolution of pneumonia complicating influenza A, the practitioners can be aware of the importance of following−up examinations by chest HRCT in monitoring and assessing the conditions, although the optimal time points for following-up examinations remain unknown.

Despite the reported findings, several limitations do exist in our study. Firstly, all the patients in our study were in patients, and, therefore, the finding was biased toward patients with severe condition. Secondly, the scanning intervals were not uniform for the patients, which was caused by the retrospective nature of this study, with no systematic assessment of all patients prospectively. Thirdly, this study failed to address the comparisons between clinical and HRCT manifestations at different time points. Such comparisons require detailed clinical and immunological data, and, therefore, can be performed when data are available. In addition, fibrosis was not histologically confirmed for the group of patients, although the signs by HRCT scanning are convincing. Finally, based on the limited size of sampling, the full diseases spectrum failed to be fully demonstrated.

5. Conclusion

In summary, this study provides HRCT evidence of pulmonary improvement in patients who are progressing and recovering from the acute stage of pneumonia complicating influenza A (H1N1) that is potentially fatal. The lung parenchymal abnormalities on HRCT improve considerably within the initial 14 days of illness. Thereafter, these abnormalities predominantly develop into fibrosis. The longitudinal follow-ups by HRCT can serve as a useful tool to assess pulmonary changes and sequelae in patients recovering from pneumonia complicating influenza A (H1N1).

References

[1] World Health Organization. Global alert and response: pandemic (H1N1) 2009: update 112. Geneva: World Health Organization; 2009. http://www.who.int/csr/don/2010-08-06/en/index.html.

[2] Liu L, Zhang RF, Lu HZ, Lu SH, Huang Q, Xiong YY, et al. Sixty-two severe and critical patients with 2009 influenza A (H1N1) in Shanghai, China. Chin Med J Engl 2011;124(11):1662−6.
[3] Lazoura O, Parthipun AA, Roberton BJ, Roberton BJ, Downey K, Finney S, et al. Acute respiratory distress syndrome related to influenza A H1N1 infection: correlation of pulmonary computed tomography findings to extracorporeal membrane oxygenation treatment and clinical outcome. J Crit Care 2012;27(6):602−8.
[4] Nickel KB, Marsden-Haug N, Lofy KH, Turnberg WL, Rietberg K, Lloyd JK, et al. Age as an independent risk factor for intensive care unit admission or death due to 2009 pandemic influenza A (H1N1) virus infection. Public Health Rep 2011;126(3):349−53.
[5] Laguna-Torres VA, Benavides JG. Infection and death from influenza A H1N1 virus in Mexico. Lancet 2009;374(9707):2032−3.
[6] Nicolini A, Ferrera L, Rao F, Senarega R, Ferrari-Bravo M. Chest radiological findings of influenza A H1N1 pneumonia. Rev Port Pneumol 2012;18(3):120−7.
[7] Marchiori E, Zanetti G, D'Ippolito G, Verrastro CG, Meirelles GS, Capobianco J, et al. Swine-origin influenza A (H1N1) viral infection: thoracic findings on CT. AJR Am J Roentgenol 2011;196(6):W723−8.
[8] Marchiori E, Zanetti G, Hochhegger B, Rodrigues RS, Fontes CA, Nobre LF, et al. High-resolution computed tomography findings from adult patients with Influenza A (H1N1) virus-associated pneumonia. Eur J Radiol 2010;74(1):93−8.
[9] Grieser C, Goldmann A, Steffen IG, Kastrup M, Fernandez CM, Engert U, et al. Computed tomography findings from patients with ARDS due to influenza A (H1N1) virus-associated pneumonia. Eur J Radiol 2012;81(2):389−94.
[10] El-Badrawy A, Zeidan A, Ebrahim MA. 64 multidetector CT findings of influenza A (H1N1) virus in patients with hematologic malignancies. Acta Radiol 2012;53(6):662−7.
[11] Marchiori E, Zanetti G, Mano CM, Hochhegger B, Irion KL. Follow-up aspects of influenza A (H1N1) virus-associated pneumonia: the role of high-resolution computed tomography in the evaluation of the recovery phase. Korean J Radiol 2010;11(5):587.
[12] Li P, Zhang JF, Xia XD, Su DJ, Liu BL, Zhao DL, et al. Serial evaluation of high-resolution CT findings in patients with pneumonia in novel swine-origin influenza A (H1N1) virus infection. Br J Radiol 2012;85(1014):729−35.
[13] Antonio GE, Wong KT, Hui DS, Wu A, Lee N, Yuen EH, et al. Thin-section CT in patients with severe acute respiratory syndrome following hospital discharge: preliminary experience. Radiology 2003;228(3):810−5.
[14] Marchiori E, Zanetti G, Fontes CA, Santos ML, Valiante PM, Mano CM, et al. Influenza A (H1N1) virus-associated pneumonia: high-resolution computed tomography-pathologic correlation. Eur J Radiol 2011;80(3):e500−504.
[15] Yuan Y, Tao XF, Shi YX, Liu SY, Chen JQ. Initial HRCT findings of novel influenza A (H1N1) infection. Influenza Other Respir Viruses 2012;6(6):e114−119.
[16] Elicker BM, Schwartz BS, Liu C, Chen EC, Miller SA, Chiu CY, et al. Thoracic CT findings of novel influenza A (H1N1) infection in immunocompromised patients. Emerg Radiol 2010;17(4):299−307.
[17] Valente T, Lassandro F, Marino M, Squillante F, Aliperta M, Muto R. H1N1 pneumonia: our experience in 50 patients with a severe clinical course of novel swine-origin influenza A (H1N1) virus (S-OIV). Radiol Med 2012;117(2):165−84.
[18] Mineo G, Ciccarese F, Modolon C, Landini MP, Valentino M, Zompatori M. Post-ARDS pulmonary fibrosis in patients with H1N1 pneumonia: role of follow-up CT. Radiol Med 2012;117(2):185−200.
[19] Mauad T, Hajjar LA, Callegari GD, Da SL, Schout D, Galas FR, et al. Lung pathology in fatal novel human influenza A (H1N1) infection. Am J Respir Crit Care Med 2010;181(1):72−9.
[20] Guo HH, Sweeney RT, Regula D, Leung AN. Best cases from the AFIP: fatal 2009 influenza A (H1N1) infection, complicated by acute respiratory distress syndrome and pulmonary interstitial emphysema. Radiographics 2010;30(2):327−33.
[21] Gill JR, Sheng ZM, Ely SF, Guinee DG, Beasley MB, Suh J, et al. Pulmonary pathologic findings of fatal 2009 pandemic influenza A/H1N1 viral infections. Arch Pathol Lab Med 2010;134(2):235−43.
[22] Chu WC, Li AM, Ng AW, So HK, Lam WW, Lo KL, et al. Thin-section CT 12 months after the diagnosis of severe acute respiratory syndrome in pediatric patients. AJR Am J Roentgenol 2006;186(6):1707−14.
[23] Qia WX, Gao S, Liu CX, Shinong P, Guo QY. Computed tomographic features of pregnant women with pandemic H1N1 virus infection. Radiol Infect Dis 2014;1(1):23−7.